(2 + 1)-D spatial ring solitons in a semiconductor quantum well system

2015 EPL 112 56002

(http://iopscience.iop.org/0295-5075/112/5/56002)

A Letters Journal Exploring the Frontiers of Physics

December 2015

EPL, **112** (2015) 56002
doi: 10.1209/0295-5075/112/56002

www.epljournal.org

(2 + 1)-D spatial ring solitons in a semiconductor quantum well system

Jibing Liu[1(a)], Tangkun Liu[1], Hong Li[1], Xiao-Tao Xie[2(b)], D. N. Wang[3] and Ray-Kuang Lee[4]

[1] *College of Physics and Electronic Science and Hubei Key Laboratory of Pollutant Analysis and Reuse Technology, Hubei Normal University - Huangshi 435002, PRC*
[2] *School of Physics and Information Technology, Shaanxi Normal University - Xi'an 710119, PRC*
[3] *College of Optical and Electronic Technology, China Jiliang University - Hangzhou 310018, PRC*
[4] *Institute of Photonics Technologies, National Tsing-Hua University - Hsinchu 300, Taiwan*

received 13 July 2015; accepted in final form 26 November 2015
published online 18 December 2015

PACS 68.65.Fg – Quantum wells
PACS 42.65.Tg – Optical solitons; nonlinear guided waves
PACS 42.70.Nq – Other nonlinear optical materials; photorefractive and semiconductor materials

Abstract – In this paper, we investigate the interaction between the semiconductor quantum well (QW) structure, a weak probe field and a strong control field. Due to the quantum interference effect induced by the strong control field, the absorption of the weak probe field is small and the Kerr nonlinearity can be greatly enhanced. The results show that the spatial soliton can form in the semiconductor QW structure via electromagnetically induced transparency (EIT). We also discuss the optical response of the system and obtain the giant $\chi^{(3)}$ and $\chi^{(5)}$ susceptibilities with opposite signs. In the one-dimension case, we obtain the analytical solutions for bright and dark spatial solitons. For a general case, we present numerical solutions for ring solitons with experimental parameters and show that the ring solitons are stable against azimuthal perturbation.

Introduction. – The concept of soliton was introduced by Zabusky and Kruskal [1], due to its shape and velocity keeping unchanged during propagation and after collisions, the study of temporal and spatial soliton has received a great deal of attention [2–15]. The research of the temporal vector optical solitons [16–18] has also been considered due to the potential applications for the design of new types of all-optical switches and logic gates. Especially, the ultra-slow two-color soliton [19,20] and temporal vector optical solitons [21] with small absorption have been studied in life-broadened four- or five-level atomic system via EIT. Ring solitons have been found in self-defocusing nonlinear media by Kivshar and Yang [22]. The ring dark solitons in Bose-Einstein condensates were introduced by Theocharis *et al.* [23], and they discussed the dynamics of the original ring soliton. The vortex ring solitons [24] were observed in Bose-Einstein condensate experiments using density engineering on the healing length scale and they showed that the oscillating solitons evolve periodically between vortex rings and solitons. Spatial solitons [25] with low light intensities can be generated in an EIT medium composed of a strong field and a four-level atomic system. And the dynamics of the weak spatial soliton can be controlled by varying the strong control field. The three-state atomic system [26] can generate (2 + 1)-D stable spatial optical solitons with extremely weak-light intensity under the EIT condition. Giant $\chi^{(3)}$ and $\chi^{(5)}$ susceptibilities [27] of opposite signs can be obtained in the atomic system through a mechanism of EIT and multidimensional solitons and light condensates can appear in this system. The formation and evolution of optical vortices can be greatly affected by the size and topological charge of the incident beam in multilevel atomic vapors [28]. In a nonlocal medium, the stability of the vector-necklace-ring soliton clusters can be adjusted by the mutual trapping of the constituent components and nonlocality [29].

Model and (1 + 1)-D analytical solution. – In this work, we study the optical response of a weak probe field and spatial soliton generation in a semiconductor QW system. Here we consider the system composed of a three-level semiconductor QW, a weak probe field and a strong control field, as shown in fig. 1. We not only show

(a) E-mail: liu0328@foxmail.com
(b) E-mail: xtxie1@gmail.com

$$\chi_p = \frac{\mu_{01}^2 N_0}{\epsilon_0 \hbar} \frac{\gamma_1[\gamma_{21}\Omega_c^2 R_3(R_1^* R_3^* - \Omega_c^2) + \Omega_c^2(2Im[M]\gamma_2\gamma_1^{-1} + \gamma_{20}R_1^*)\Omega_p^2 - \gamma_2 M(R_2^*\Omega_c^2 + R_1^* M^*)]}{\gamma_1[\Omega_c^2(N_4 - i\gamma_{21}\Omega_c^2(\Omega_c^2 - N_2)) - i\gamma_2|N_1|^2] + B\Omega_p^2 + \Omega_c^2\gamma_{10}(\gamma_2 - 3\gamma_{20} + \gamma_1 - 2\gamma_2\gamma_{21}\gamma_{10}^{-1})\Omega_p^4}, \quad (2)$$

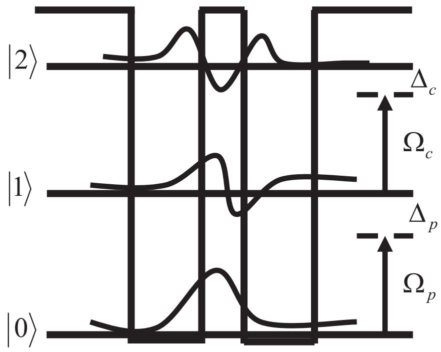

Fig. 1: Schematic of the 3-level cascade system in a quantum well system. $|j\rangle (j = 0, 1, 2)$ denote the subband states. Ω_p is the Rabi frequency of the weak probe field and drives the transition from $|0\rangle$ to $|1\rangle$, and Ω_c is the Rabi frequency of the strong coupling field and drives the transition from $|1\rangle$ to $|2\rangle$. The bare state transition energies are $E_{10} = 124$ meV and $E_{12} = 185$ meV.

that the absorption of the weak probe field can be canceled by adjusting the intensity of the strong control field, but also obtain giant $\chi^{(3)}$ and $\chi^{(5)}$ susceptibilities with opposite signs in the QW medium. A few works have focused on the coherent control of intersubband transitions in QW, such as laser-induced quantum coherence [30], AC stark splitting and quantum interference [31], slow temporal optical solitons [32] in QW, optical bistability [33] via intersubband transitions in QW. Our present work is different from those studies as we focused on the generation and stability of (2 + 1)-D spatial solitons.

The present semiconductor QW sample is very much similar to the one reported in refs. [30,31], which has been grown by the molecular beam epitaxy method. This sample consists of 50 periods, each with a 4.8 nm $In_{0.47}Ga_{0.53}As$/0.2 nm $Al_{0.48}In_{0.52}As$/4.8 nm $In_{0.47}Ga_{0.53}As$, separated by modulation-doped 36 nm $Al_{0.48}In_{0.52}As$ barriers. For this case, the semiconductor QW can be recognized as a three-level system with the subband energy levels $|0\rangle$, $|1\rangle$ and $|2\rangle$, respectively. The corresponding transition frequencies are $\omega_{01} = 124$ meV, and $\omega_{12} = 185$ meV, respectively. The weak probe field $E_p e^{i\omega_p t}$ drives the transition from $|0\rangle$ to $|1\rangle$ and the strong coupling field $E_c e^{i\omega_c t}$ drives the transition from $|1\rangle$ to $|2\rangle$. We suppose the frequencies of probe and coupling fields are close to the transition frequencies, *i.e.* $|\omega_p - \omega_{01}|/\omega_{01} \ll 1$ and $|\omega_c - \omega_{12}|/\omega_{12} \ll 1$, respectively. The Rabi frequencies are defined as $\Omega_{p(c)} = \mu_{01(12)}E_{p(c)}/\hbar$. Here $\mu_{01(12)}$ is the dipole moment for the intersubband transition from $|0\rangle$ to $|1\rangle$ ($|1\rangle$ to $|2\rangle$). It is noted that the dynamics of the system can be described by the Liouville equation. Under the rotating wave approximation, the equation of motion for the density matrix element ρ_{ij} can be written as

$$\dot{\rho_{11}} = -\gamma_1\rho_{11} + \gamma_2\rho_{22} + i(\Omega_p\rho_{01} - \Omega_p^*\rho_{10} + \Omega_c^*\rho_{21} - \Omega_c\rho_{12}), \quad (1a)$$

$$\dot{\rho_{00}} = \gamma_1\rho_{11} - i(\Omega_p\rho_{01} - \Omega_p^*\rho_{10}), \quad (1b)$$

$$\dot{\rho_{10}} = iR_1\rho_{10} + i\Omega_c^*\rho_{20} + i\Omega_p(\rho_{00} - \rho_{11}), \quad (1c)$$

$$\dot{\rho_{21}} = iR_2\rho_{21} + i\Omega_c(\rho_{11} - \rho_{22}) - i\Omega_p^*\rho_{20}, \quad (1d)$$

$$\dot{\rho_{20}} = iR_3\rho_{20} - i\Omega_p\rho_{21} + i\Omega_c\rho_{10}, \quad (1e)$$

along with the corresponding complex conjugates $\rho_{ij} = \rho_{ji}^*(j \neq i)$ and the conservation condition $\rho_{00} + \rho_{11} + \rho_{22} = 1$. Here $R_1 = \Delta_p + i\gamma_{10}/2$, $R_2 = \Delta_c + i\gamma_{21}/2$, $R_3 = \Delta_p + \Delta_c + i\gamma_{20}/2$, the single photon detunings are defined as $\Delta_p = \omega_p - \omega_{01}$ and $\Delta_c = \omega_c - \omega_{12}$. The population decay rates, which correspond to subband states $|1\rangle$ and $|2\rangle$, are denoted as γ_1 and γ_2. And the total decay rates are defined as $\gamma_{10} = \gamma_1 + \gamma_{10}^{dph}$, $\gamma_{20} = \gamma_2 + \gamma_{20}^{dph}$, and $\gamma_{21} = \gamma_1 + \gamma_2 + \gamma_{21}^{dph}$, where γ_{ij}^{dph} denotes the dephasing decay rate, which comprises the sum of the quasielastic acoustic phonon scattering and the elastic interface roughness scattering, and the dephasing decay rate can be estimated according to refs. [31,34].

The susceptibility is defined as $\chi_p = N_0\mu_{10}\rho_{10}/\epsilon_0 E_p$, where N_0 is the electron density in the conduction band of the QW and ϵ_0 is the permittivity of free space. With the help of eq. (1) at the steady-state case, the analytical expression for the susceptibility can be obtained as

see eq. (2) *above*

where $N = R_1R_2R_3$, $N_1 = N - R_2\Omega_c^2 - R_1\Omega_p^2$, $N_2 = 2i\text{Im}[NR_2^{-1}]$, $N_3 = -2i\text{Im}[N(1 + R_2^*R_1^{-1})]$, $N_4 = -2i\text{Im}[R_2^{-1}]$, $B = \Omega_c^4(\gamma_{21}(\gamma_2 - 3\gamma_{20}) - \gamma_1(\gamma_{10} + \gamma_{21})) - \Omega_c^2(\gamma_1 N_3 + i\gamma_2 N_3 - 3|R_3|^2\gamma_{10}\gamma_{21}) - 2\gamma_2\gamma_{10}|M|^2$ and $M = R_2R_3 - \Omega_p^2$. In order to describe the high-order nonlinear optical response of the semiconductor QW structure, we express the susceptibility as a power series in the field strength E_p, such as $\chi = \sum_{j=0}^{j=\infty} \chi^{2j+1}|E_p|^{2j}$, then we obtain

$$\chi^{(1)} = \frac{\mu_{01}^2 N_0}{\epsilon_0\hbar}\frac{3R_3}{\Omega_c^2 - R_1R_3}, \quad (3a)$$

$$\chi^{(3)} = \frac{\mu_{01}^2}{\hbar^2}\chi^{(1)} \times\left(\frac{\Omega_c^2 R_{23}^I\gamma_2 + \gamma_1(R_1^*\gamma_{20}\Omega_c^2 - \gamma_2(R_1^*R_{23}^R - R_2^*\Omega_c^2))}{3R_3\gamma_1(R_1^*R_3^* - \Omega_c^2)(|R_2|^2\gamma_2 + \gamma_{21}\Omega_c^2)} - \frac{B_1}{B_0}\right), \quad (3b)$$

$$\chi^{(5)} = \chi^{(1)}\frac{\mu_{01}^4}{\hbar^4}\left(\frac{\gamma_2 R_1^*}{3R_3(R_1^*R_3^* - \Omega_c^2)(|R_2|^2\gamma_2 + \gamma_{21}\Omega_c^2)} - \frac{B_1}{B_0}\frac{\chi^{(3)}}{\chi^{(1)}}\frac{\hbar^2}{\mu_{01}^2} - \frac{B_2}{B_0}\right), \quad (3c)$$

with

$$B_0 = \gamma_1(R_1R_3-\Omega_c^2)(\Omega_c^2-R_1^*R_3^*)(\gamma_2|R_2|^2+\gamma_{21}\Omega_c^2), \quad (4a)$$
$$B_1 = \gamma_2(2\gamma_{10}|R_2R_3|^2 + R_1\Omega_c^4 + \gamma_{21}\Omega_c^4 + \gamma_1(|R_1|^2R_{23}^R - R_{12}^R|\Omega_c|^2)) + T_0, \quad (4b)$$
$$B_2 = -\gamma_{10}(\gamma_1 + 3\gamma_{20})\Omega_c^2 + \gamma_2(2\gamma_{10}R_{23}^R - |R_1|^2\gamma_1 + (\gamma_{10} - 2\gamma_{21})\Omega_c^2), \quad (4c)$$

where $T_0 = \Omega_c^2(\gamma_1(R_0 - (\gamma_{21} + \gamma_{10})\Omega_c^2) - 3\gamma_{21}(\gamma_{10}|R_3|^2 + \gamma_{20}\Omega_c^2))$, $R_0 = \gamma_{10}\Delta_c^2 + (\gamma_{10} + \gamma_{20} + \gamma_{21})\Delta_c\Delta_p + (\gamma_{21} - \gamma_{20})\Delta_p^2 - 0.25\gamma_{10}^2\gamma_{20} - 0.25\gamma_{10}\gamma_{20}\gamma_{21}$, $R_4 = -\gamma_{21}\Delta_p^2 - (\gamma_{10} + \gamma_{20} + \gamma_{21})\Delta_c\Delta_p - (\gamma_{10} + 2\gamma_{20})\Delta_c^2 - 0.5\gamma_{21}^2\gamma_{20} - 0.25\gamma_{10}\gamma_{20}\gamma_{21}$, $R_{23}^I = \gamma_{20}\Delta_c + \gamma_{21}\Delta_c + \gamma_{21}\Delta_p$, $R_{23}^R = 2\Delta_c^2 + 2\Delta_c\Delta_p - 0.5\gamma_{20}\gamma_{21}$. Figure 2 shows the relationship between the real and imaginary parts of the susceptibility χ and the square of the probe field's Rabi frequency $|\Omega_p|^2$. According to the separate absorption saturation intensity measurement [35], the population decay rate γ_1 from state $|1\rangle$ to $|0\rangle$ is 1.3 meV and the population decay rate γ_2 is 0.9 meV, so the overall decay rate [31] is $\gamma_{10} \sim \gamma_{21} \sim$ 5 meV. Since the transition from $|2\rangle$ to $|0\rangle$ is dipole forbidden, the dephasing decay rate $\gamma_{20}^{dph} \ll \gamma_{10}^{dph}(\gamma_{21}^{dph})$, and hence $\gamma_{20} \sim \gamma_2 \sim 1.3$ meV. Since the present study focuses only on the low temperatures up to 10 K, the sheet electron density of semiconductor QW structure is $\sim 4\times10^{11}$ cm^{-2}. From fig. 2, we see that the imaginary part of the susceptibility is much smaller than the real part. This indicates that the absorption of the probe field in our system is small. The real part of the susceptibility is proportional to the probe field's intensity for low powers, while it decreases when the probe field's intensity increases for high powers. Moreover the real part of the third-order susceptibility $\chi_r^{(3)}$ is positive, while the real part of the fifth-order susceptibility $\chi_r^{(5)}$ is negative. Figure 2 indicates that the semiconductor QW structure considered here presents a nonlinear self-focusing for low powers and a nonlinear self-defocusing for high powers. The nonlinear property in the semiconductor QW structure is similar to the cubic-quintic nonlinear property in other media [27,36–43]. Due to giant $\chi^{(3)}$ and $\chi^{(5)}$ susceptibilities with opposite signs, the stable two-dimensional liquid light condensates [27] have been shown in an atomic system via EIT. Rarefaction pulses [38] can be generated by soliton-soliton interference in a cubic-(focusing-)quintic (defocusing) nonlinear system. Highly efficient four-wave mixing and six-wave mixing processes [39] have been generated in atomic systems and the coexistence of four-wave mixing and six-wave mixing processes can be used to estimate the coefficient $\chi^{(5)}$.

We assume that the coupling field's Rabi frequency satisfies $\Omega_c \gg \gamma_{20}\gamma_{10}$ and $\Omega_c \gg \Omega_p$. For the resonance case ($\Delta_p = \Delta_c = 0$), we can obtain $\mathrm{Im}[\chi^{(1)}] \propto \frac{\mu_{01}^2 N_0}{\epsilon_0\hbar}\frac{\gamma_{20}}{\Omega_c^2}$. So the strong coupling field Ω_c can efficiently suppress the absorption of the weak probe field Ω_p. Because of the effects of EIT, the weak probe field E_p can propagate in the semiconductor QW system without absorption, which is governed by the Maxwell equation

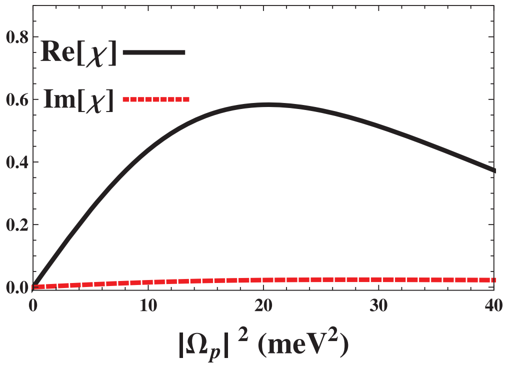

Fig. 2: (Color online) The real and imaginary parts of the susceptibility χ as a function of the square of the probe field's Rabi frequency $|\Omega_p|^2$, the parameters are given in the main text.

$$\nabla^2\vec{E}_p - \frac{1}{c^2}\frac{\partial^2\vec{E}_p}{\partial t^2} = \frac{1}{\epsilon_0 c^2}\frac{\partial^2\vec{P}}{\partial t^2}, \quad (5)$$

where c is the velocity of light in vacuum. We assume a linear relationship between $\vec{P}$ and $\vec{E}$, so we obtain $\vec{P} = \epsilon_0\chi E$. Assuming the amplitude of the probe field varying slowly along the z-direction, the propagation equation of the probe field in this semiconductor QW medium is given by

$$2ik_p\frac{\partial E_p}{\partial z} + \nabla_\perp^2 E_p = -k_p^2\chi_p E_p, \quad (6)$$

where $\nabla_\perp^2$ is the transverse Laplacian operator, k_p and E_p are the wave number and amplitude of the probe field. Substituting eqs. (3a)–(3c) into eq. (6), we obtain

$$2ik_p\frac{\partial E_p}{\partial z} + \nabla_\perp^2 E_p + k_p^2\sum_{j=0}^{j=2}\chi_p^{(2j+1)}|E_p|^{2j}E_p = 0, \quad (7)$$

Since the optical susceptibility χ is complex, we can write $\chi^{(1)} = \chi_r^{(1)} + i\chi_i^{(1)}$, $\chi^{(3)} = \chi_r^{(3)} + i\chi_i^{(3)}$, and $\chi^{(5)} = \chi_r^{(5)} + i\chi_i^{(5)}$. If a reasonable and realistic set of parameters can be satisfied that $\chi_r^{(1)} \gg \chi_i^{(1)}$, $\chi_r^{(3)} \gg \chi_i^{(3)}$, and $\chi_r^{(5)} \gg \chi_i^{(5)}$, we obtain $\chi^{(1)} \simeq \chi_r^{(1)}$, $\chi^{(3)} \simeq \chi_r^{(3)}$, and $\chi^{(5)} \simeq \chi_r^{(5)}$. Assuming the probe field is very small, the optical susceptibility χ can expressed as

$$\chi \simeq \chi^{(1)} + \chi^{(3)}|E_p|^2, \quad (8)$$

For the case of $(1+1)$-dimensional probe fields, substituting eq. (8) into eq. (6), we obtain

$$2ik_p\frac{\partial E_p}{\partial z} + \frac{\partial^2}{\partial x^2}E_p + k_p^2(\chi_p^{(1)} + \chi_p^{(3)}|E_p|^2)E_p = 0, \quad (9)$$

Equation (9) admits a solution describing bright solitons ($\chi^{(3)} > 0$) and dark solitons ($\chi^{(3)} < 0$), the fundamental bright soliton is given by

$$E_p = E_0\mathrm{sech}(x/\tau)\exp[i0.5k_p(E_0^2\chi_p^{(3)} + \chi_p^{(1)})z], \quad (10)$$

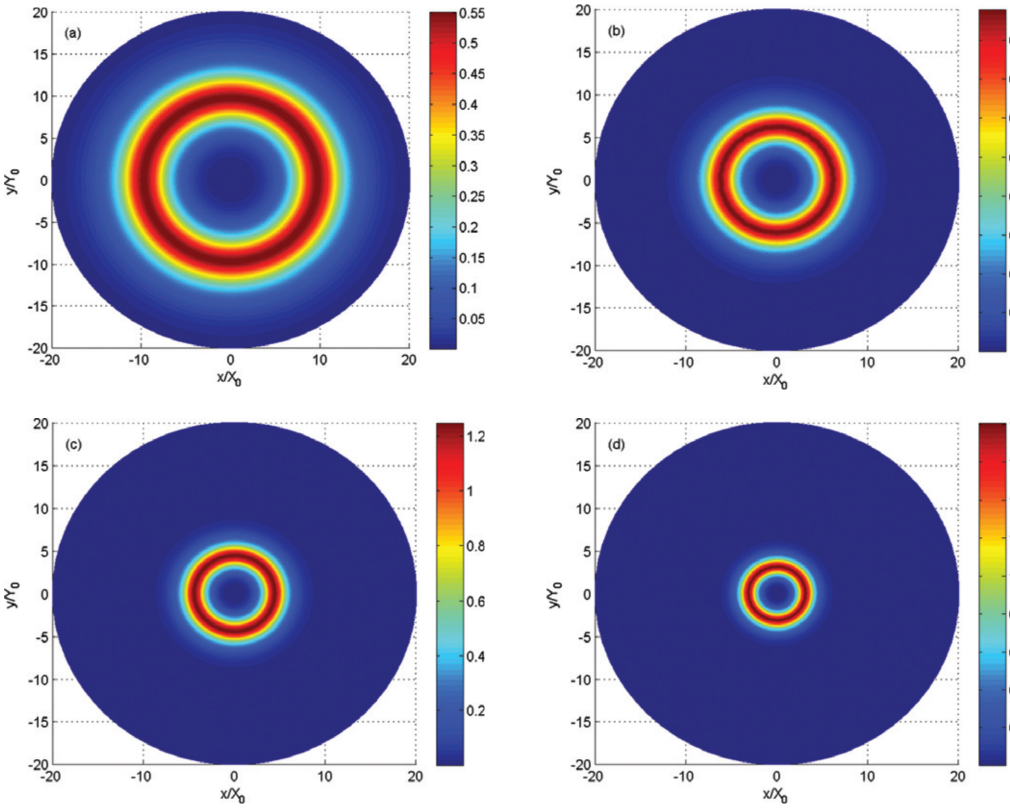

Fig. 3: (Color online) The solution forms of the ring solitons with vortex charge $m = 3$ and propagation constant $\beta = 0.1, 0.25, 0.5$ and 1 are shown in panels (a)–(d), respectively, $X_0 = Y_0 = 1 \times 10^{-6}$ m.

where $\tau = (\sqrt{0.5\chi_p^{(3)}}k_pE_0)^{-1}$ with the amplitude E_0 which is related to the full width at half maximum (FWHM) $x_{FWHM} = 2\sqrt{2}\ln(2+\sqrt{3})\sqrt{\chi_p^{(3)}}/k_pE_0$. It is noted that the width of the soliton is determined by the amplitudes of probe and coupling fields and the detunings δ_c and Δ_p. We can tune the coupling field's amplitude and the detunings to achieve no absorption. So the width of the soliton does not change when it propagates in this semiconductor QW medium. When ($\chi^{(3)} < 0$), the fundamental dark soliton is given by

$$E_p = E_0 \tanh(x/\tau)\exp[i0.5k_p(E_0^2\chi_p^{(3)} + \chi_p^{(1)})z]. \quad (11)$$

Numerical solution of ring solitons. – For a $(2+1)$-D nonlinear Schrödinger equation, it is difficult to find the analytical solution. Next, we will present a numerical solution for eq. (7). For simplicity, we use the polar coordinates instead of the rectangular coordinates. We assume the stationary transverse solutions in eq. (7) of the form $E_p(r,\theta,z) = \phi_m(r)e^{i\beta z + im\theta}$, where β is the propagation constant, $m = 0, \pm1, \pm2, \ldots$, for $m \neq 0$, this solution is related to vortex solitons. In polar coordinates, we can derive the following equation:

$$\left[\frac{\mathrm{d}^2}{\mathrm{d}r^2} + \frac{1}{r}\frac{\mathrm{d}}{\mathrm{d}r} - \frac{m^2}{r^2} - 2k_p\beta + k_p^2\sum_{j=0}^{j=2}\chi_p^{(2j+1)}|\phi_m|^{2j}\right] \times \phi_m(r) = 0, \quad (12)$$

with the boundary conditions $\phi_m(r = \infty) = 0$ and $\phi_m'(r = 0) = 0$. We now present numerical results to illustrate the existence of ring solitons in this QW system. According to the experimental in refs. [30,31], the sheet electron density is $4 \times 10^{11}\,\mathrm{cm}^{-2}$, $\gamma_1 \simeq 1.3\,\mathrm{meV}$, $\gamma_{20} \simeq 0.9\,\mathrm{meV}$ and $\gamma_{10} \simeq \gamma_{21} = 5\,\mathrm{meV}$, $\Delta_p = 36.5\,\mathrm{meV}$ and $\Omega_c = 50\,\mathrm{meV}$, we can obtain $\chi^{(1)} \simeq 0.23 + 0.026i \simeq 0.23$, $\chi^{(3)} \simeq -1 \times 10^{-3} - 1 \times 10^{-4}i \simeq -0.001$ and $\chi^{(5)} \simeq 3.9 \times 10^{-5} + 4.3 \times 10^{-6}i \simeq 3.9 \times 10^{-5}$. For $m = 3$ and different values of β, we numerically search the computed spatial profile $\phi_m(r)$ which satisfies the given boundary conditions in eq. (12). The numerical solutions with different profiles which correspond to different $\beta = 0.1, 0.25, 0.5$ and $1\,\mu\mathrm{m}^{-1}$ have been presented in fig. 3. From fig. 3, we see that the height of the ring soliton becomes higher with increasing the propagation constant β and the radius of the ring soliton is inversely proportional to the propagation constant β.

The power of ring solitons can be defined as $P = \int\int \phi_m^2 \mathrm{d}x\mathrm{d}y$. In order to test the stability of $(2+1)$-D ring solitons against small perturbations, we plot the relation between the power of a ring soliton and the propagation constant β for $m = 3$ in fig. 4. Figure 4 shows that the power of ring solitons is proportional to the propagation constant β. We find that the inequality $\frac{\mathrm{d}P}{\mathrm{d}\beta} > 0$ is satisfied in each point of the curve in fig. 4. It is very important to determine the stability of the ring soliton solution and

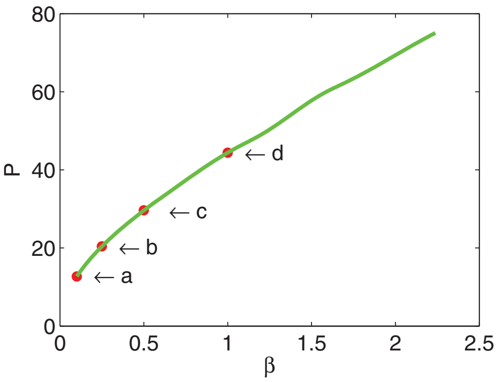

Fig. 4: (Color online) The relation between the power and propagation constant for the ring soliton solution.

many studies [44–48] focused on this problem with different methods. In order to test the stability of the ring soliton solutions, we simulate directly the propagation of our solutions with eq. (7), which shows that the solutions in fig. 3 are stable against azimuthal perturbation.

Conclusion. – We studied theoretically optical phenomena in a semiconductor QW system which interact with a weak probe field and a strong control field. Using the density matrix method, we have obtained the analytical expression for susceptibility at a steady case. It is found that the imaginary part of susceptibility is much smaller than the real part in some conditions. In this case, the probe field's absorption is very small. We also obtained the giant $\chi^{(3)}$ and $\chi^{(5)}$ susceptibilities with opposite signs. And we presented the ring spatial soliton solution in a numerical form. At last, we investigated the relationship between the power P and propagation constant β and the numerical results show that the ring spatial soliton solutions are stable against azimuthal perturbation.

* * *

The research is supported in part by the National Basic for Research Program of China (No. 2012CB922103), and by the NNSF of China (Nos. 11547195, 11274104, and 91021011) and by the Scientific and Technological Research Program of Education Department of Hubei Province (Nos. Z200722001, 2015CFB535, and D20152501). The authors acknowledge Prof. Ying Wu for his enlightening suggestions.

REFERENCES

[1] Zabusky N. J. and Kruskal M. D., *Phys. Rev. Lett.*, **15** (1965) 24017.
[2] Agrawal G. P., *Nonlinear Fiber Optics* (Academic Press, New York) 2001, Chapt. 5.
[3] Haus H. A. and Wong W. S., *Rev. Mod. Phys.*, **68** (1996) 423.
[4] Wu Y. and Deng L., *Phys. Rev. Lett.*, **93** (2004) 143904.
[5] Rybin A. V., Vadeiko I. P. and Bishop A. R., *Phys. Rev. E*, **72** (2005) 026613; Huang G., Deng L. and Hang C., *Phys. Rev. E*, **72** (2005) 036621.
[6] Liu X.-J., Jing H. and Ge M.-L., *Phys. Rev. A*, **70** (2004) 055802.
[7] Xie X.-T., Li W.-B. and Yang X., *J. Opt. Soc. B*, **23** (2006) 1609.
[8] Xie X.-T., Li W., Li J., Yang W. X., Yuan A. and Yang X., *Phys. Rev. B*, **75** (2007) 184423; Liu J.-B., Xie X.-T. and Wu Y., *EPL*, **89** (2010) 17006.
[9] Wu Y. and Yang X., *Appl. Phys. Lett.*, **91** (2007) 094104.
[10] Wu B., Liu J. and Niu Q., *Phys. Rev. Lett.*, **88** (2002) 034101.
[11] Salasnich L. and Malomed B. A., *Phys. Rev. A*, **74** (2006) 053610.
[12] Nistazakis H. E., Frantzeskakis D. J., Kevrekidis P. G., Malomed B. A. and Carretero-González R., *Phys. Rev. A*, **77** (2008) 033612.
[13] Xiong H., Liu S., Huang G. and Xu Z., *J. Phys. B*, **35** (2002) 4863.
[14] Adamashvili G. T., Weber C., Knorr A. and Adamashvili N. T., *Phys. Rev. A*, **75** (2007) 063808.
[15] Yang W.-X., Hou J.-M. and Lee R.-K., *Phys. Rev. A*, **77** (2008) 033838.
[16] Christodoulides D. N. and Joseph R. I., *Opt. Lett.*, **13** (1988) 53.
[17] Barad Y. and Silberberg Y., *Phys. Rev. Lett.*, **78** (1997) 3290.
[18] Rand D., Glesk I., Brès C.-S., Nolan D. A., Chen X., Koh J., Fleischer J. W., Steiglitz K. and Prucnal P. R., *Phys. Rev. Lett.*, **98** (2007) 053902.
[19] Deng L., Payne M. G., Huang G. and Hagley E. W., *Phys. Rev. E*, **72** (2005) 055601(R).
[20] Wu Y., *Phys. Rev. A*, **71** (2005) 053820.
[21] Si L.-G., Yang W.-X., Liu J.-B., Li J. and Yang X., *Opt. Express*, **17** (2009) 7771.
[22] Kivshar Y. S. and Yang X., *Phys. Rev. E*, **50** (1994) R40.
[23] Theocharis G., Frantzeskakis D. J., Kevrekidis P. G., Malomed B. A. and Kivshar Y. S., *Phys. Rev. Lett.*, **90** (2003) 120403.
[24] Shomroni I., Lahoud E., Levy S. and Steinhauer J., *Nat. Phys.*, **5** (2009) 193.
[25] Hong T., *Phys. Rev. Lett.*, **90** (2003) 183901.
[26] Hang C., Huang G. and Deng L., *Phys. Rev. E*, **74** (2006) 046601.
[27] Michinel H., Paz-Alonso M. J. and Perez-Garcia V. M., *Phys. Rev. Lett.*, **96** (2006) 023903.
[28] Zhang Y., Wu Z., Yuan C., Yao X., Lu K., Belic M. and Zhang Y., *Opt. Lett.*, **37** (2012) 4507.
[29] Shen M., Kong Q., Jeng C. C., Ge L. J., Lee R. K. and Krolikowski W., *Phys. Rev. A*, **83** (2011) 023825.
[30] Serapiglia G. B., Paspalakis E., Sirtori C., Vodopyanov K. L. and Phillips C. C., *Phys. Rev. Lett.*, **84** (2000) 1019.
[31] Dynes J. F., Frogley M. D., Beck M., Faist J. and Phillips C. C., *Phys. Rev. Lett.*, **94** (2005) 157403.
[32] Yang W.-X. and Lee R. K., *EPL*, **83** (2008) 14002.
[33] Li J.-H., *Phys. Rev. B*, **75** (2007) 155329.
[34] Schmidtetal H., *Appl. Phys. Lett.*, **70** (1997) 3455.
[35] Slivken S., Litvinov V. I., Razeghi M. and Meyer J. R., *J. Appl. Phys.*, **85** (1999) 665.

[36] Falcao-Filho E. L., de Araújo C. B., Boudebs G., Leblond H. and Skarka V., *Phys. Rev. Lett.*, **110** (2013) 013901.

[37] Reyna A. S., Malomed B. A. and de Araújo C. B., *Phys. Rev. A*, **92** (2015) 033810.

[38] Paredes A., Feijoo D. and Michinel H., *Phys. Rev. Lett.*, **112** (2014) 173901.

[39] Zhang Y., Brown A. W. and Xiao M., *Phys. Rev. Lett.*, **99** (2007) 123603.

[40] Mihalache D., Mazilu D., Crasovan L.-C., Towers I., Buryak A. V., Malomed B. A., Torner L., Torres J. P. and Lederer F., *Phys. Rev. Lett.*, **88** (2002) 073902.

[41] Malomed B. A., Crasovan L.-C. and Mihalache D., *Physica D*, **161** (2002) 187.

[42] Greenberg J. A. and Gauthier D. J., *EPL*, **98** (2012) 24001.

[43] Zhang Y., Wu Z., Yuan C., Yao X., Lu K., Belic M. and Zhang Y., *Opt. Lett.*, **37** (2012) 4507.

[44] Pego R. L. and Warchall H. A., *J. Nonlinear Sci.*, **12** (2002) 347.

[45] Malomed B. A., Mihalache D., Wise F. and Torner L., *J. Opt. B: Quantum Semiclass. Opt.*, **7** (2005) R53.

[46] Caplan R. M., Hoq Q. E., Carretero-Gonzalez R. and Kevrekidis P. G., *Opt. Commun.*, **282** (2009) 1399.

[47] Crasovan L.-C., Malomed B. A. and Mihalache D., *Phys. Rev. E*, **63** (2000) 016605.

[48] Vakhitov N. G. and Kolokolov A. A., *Radiophys. Quantum Electron.*, **16** (1975) 783.